Check for updates

Diagnostics Accuracy of Magnetic Resonance Imaging in Detection of Atherosclerotic Plaque Characteristics in Carotid Arteries Compared to Histology: A Systematic Review

David Pakizer, MSc,[1] Jiří Kozel, MSc,[1] Jolanda Elmers, MSc,[2] Janusz Feber, MD,[1,3] Patrik Michel, MD,[4] David Školoudík, MD, PhD,[1] and Gaia Sirimarco, MD, PhD[4,5]*

Carotid plaque composition represents one of the main risk factors of future ischemic stroke. MRI provides excellent soft tissue contrast that can distinguish plaque characteristics. Our objective was to analyze the diagnostic accuracy of MRI imaging in the detection of carotid plaque characteristics compared to histology in patients with symptomatic and asymptomatic carotid atherosclerosis through a systematic review. After prospective registration in PROSPERO (ID CRD42022329690), Medline Ovid, Embase.com, Cochrane Library, and Web of Science Core were searched without any search limitation up to May 27, 2022 to identify eligible articles. Of the 8168 studies, 53 (37 × 1.5 T MRI, 17 × 3 T MRI) evaluated MRI accuracy in the detection of 13 specific carotid plaque characteristics in 169 comparisons. MRI demonstrated high diagnostic accuracy for detection of calcification (3 T MRI: mean sensitivity 92%/mean specificity 90%; 1.5 T MRI: mean sensitivity 81%/mean specificity 91%), fibrous cap (1.5 T: 89%/87%), unstable plaque (1.5 T: 89%/87%), intraplaque hemorrhage (1.5 T: 86%/88%), and lipid-rich necrotic core (1.5 T: 89%/79%). MRI also proved to have a high level of tissue discrimination for the carotid plaque characteristics investigated, allowing potentially for a better risk assessment and follow-up of patients who may benefit from more aggressive treatments. These results emphasize the role of MRI as the first-line imaging modality for comprehensive assessment of carotid plaque morphology, particularly for unstable plaque.
Evidence Level: 2
Technical Efficacy: Stage 2

J. MAGN. RESON. IMAGING 2025;61:1067–1093.

Carotid atherosclerosis constitutes an important cause of ischemic stroke, mainly of thromboembolic origin.[1,2] A growing plaque narrows the artery and causes a perfusion defect.[3] However, thrombosis is associated with rupture or erosion of a complicated lesion, highlighting that the plaque composition can play a key role in developing future ischemic stroke.[2,4]

The development of magnetic resonance imaging (MRI) allowed the detection of the carotid plaque composition due to the relatively large vessel size and its superficial location[5] and became another noninvasive modality that is feasible to reveal the plaque content in addition to ultrasound (US) and computed tomography (CT).[6] Furthermore, MRI provides excellent soft tissue contrast that differentiates plaque

View this article online at wileyonlinelibrary.com. DOI: 10.1002/jmri.29522

Received Apr 17, 2024, Accepted for publication Jun 17, 2024.

*Address reprint requests to: G.S., Centre hospitalier de Rennaz, Route du Vieux-Séquoia 20, 1847 Rennaz, Switzerland. E-mail: gaia.sirimarco@hopitalrivierachablais.ch

From the [1]Centre for Health Research, Department of Clinical Neurosciences, Faculty of Medicine, University of Ostrava, Ostrava, Czech Republic; [2]Medical Library, Lausanne University Hospital and University of Lausanne, Lausanne, Switzerland; [3]Division of Nephrology, Department of Pediatrics, Children's Hospital of Eastern Ontario, University of Ottawa, Ottawa, Ontario, Canada; [4]Stroke Center, Service of Neurology, Department of Clinical Neurosciences, Lausanne University Hospital, Lausanne, Switzerland; and [5]Neurology Unit, Department of Internal Medicine, Riviera Chablais Hospital, Rennaz, Switzerland

Additional supporting information may be found in the online version of this article

This is an open access article under the terms of the Creative Commons Attribution-NonCommercial-NoDerivs License, which permits use and distribution in any medium, provided the original work is properly cited, the use is non-commercial and no modifications or adaptations are made.

© 2024 The Author(s). *Journal of Magnetic Resonance Imaging* published by Wiley Periodicals LLC on behalf of International Society for Magnetic Resonance in Medicine.

characteristics based on biophysical and biochemical parameters (diffusion, concentration, chemical composition, physical state) and became the first noninvasive modality that allows discrimination of lipid-rich necrotic core (LRNC), intraplaque hemorrhage (IPH), fibrous cap, and other carotid plaque characteristics.[7]

Several meta-analyses confirmed a strong association between stroke risk and MRI-detected LRNC (hazard ratio [HR] 3.00), thin/ruptured fibrous cap (HR 5.93),[8] high-risk plaque characteristics in asymptomatic stenosis (odds ratio [OR] 3.00)[9] and most importantly IPH in asymptomatic (HR 7.9) and symptomatic patients (HR 10.2).[10] To use information on plaque morphology and stroke prediction for patient monitoring, risk stratification, evaluation of treatment effect, and other purposes, solid evidence on accurate detection of such characteristics by MRI is needed. However, to our knowledge, a comprehensive study evaluating available evidence on MRI diagnostic accuracy is lacking. Therefore, our objective was to analyze the diagnostic accuracy of MRI imaging in the detection of carotid plaque characteristics compared to histology in patients with symptomatic and asymptomatic carotid atherosclerosis through a systematic review.

Materials and Methods

Our study was prospectively registered on the International Prospective Register of Systematic Reviews (PROSPERO; ID CRD42022329690). Preferred Reporting Items for Systematic Reviews and Meta-analyses (PRISMA)[11] and Standards for Reporting of Diagnostic Accuracy Studies (STARD) 2015[12] guidelines were used to report the results.

We included original prospective or retrospective studies of adult patients (≥18 years) with symptomatic or asymptomatic extracranial carotid atherosclerosis detected by MRI (index test) to evaluate carotid plaque composition compared to true (nonvirtual) histological plaque evaluation (reference standard). For data extraction, studies had to report diagnostic accuracy (sensitivity and specificity) of MRI in the detection of specific plaque features or clearly stated data that allowed calculating sensitivity and specificity (true positive [TP], true negative [TN], false positive [FP], and false negative [FN]). Non-original studies without presenting new results including systematic reviews, studies that used virtual histology or visual plaque evaluation as a reference standard, and studies that published the same comparisons repeatedly (duplicate results) were excluded (Fig. 1).

A medical librarian (J.E.) prepared a comprehensive search strategy based on a combination of controlled keywords and free-text terms related to the aim of our study for search in four major databases: Medline Ovid ALL, Embase.com, Central—Cochrane Library Wiley, and Web of Science Core collection. A supplemental search was conducted in Google Scholar (with an adjusted search strategy, screening of the first 500 results) and citations of key studies were searched. Designed equations were used for search without any search limitation (eg, language or publication year) up to May 27, 2022 and are available online.[13] All duplicates were removed manually in EndNote and results were imported to the Rayyan web application (Qatar Computing Research Institute, Doha, Qatar; https://rayyan.ai/) for screening. Two independent reviewers (D.P., J.K.) manually screened all identified studies in three phases (title/abstract, full manuscript, and during data extraction) in blind mode and resolved all disagreements by consensus or independent decision of the senior team member (P.M, D.Š.).

Data extraction which focused mainly on collecting the necessary data to calculate the diagnostic accuracy (specificity, sensitivity, TP, TF, FP, FN) of the various outcomes (specific plaque characteristics), was carried out manually by two reviewers (D.P., J.K.) blinded to each other. Plaque characteristics retrieved from included studies were divided into groups by histological plaque feature. If only one study evaluated a specific characteristic, the study was included in the group "other characteristics." If a study described a characteristic such as IPH and/or LRNC by histology (combined), the study was included in the unstable plaque group. In general, 13 plaque groups were established: IPH, LRNC, calcification, fibrous plaque, fibrous cap, ulceration, neovascularization, inflammation, loose matrix, unstable plaque, and other characteristics.

All signal intensities (hyperintense, isointense, hypointense) of specific carotid plaque characteristics described in the manuscript were compared to the intensity of adjacent sternocleidomastoid muscle (used as a reference).

Results

Of the 8168 studies, 53 evaluated the diagnostic accuracy of MRI in the detection of 13 carotid plaque characteristics and were included in the systematic review (Tables 1–11). The authors of 53 retrieved studies often investigated several characteristics or sequences in a single study. Therefore, a final 169 comparisons of diagnostic accuracy were extracted and reviewed, as presented in Table S1 in the Supplemental Material.

Of the studies published from 1996 to 2022, 17 studies used 3 T magnetic field (63 comparisons of diagnostic accuracy) and 37 studies 1.5 T magnetic field (106 comparisons). Despite the wide range of publications, diagnostic accuracy did not change significantly over time, but a slight increase (<10%) in sensitivity and a decrease in specificity over time was observed for both 1.5 T MRI and 3 T MRI (Figs. S1 and S2 in the Supplemental Material). Only one study was published in the last century.[14]

Sequence Parameters

Receive-only phased array surface coils (usually 4- or 8-channel), usually dedicated bilateral carotid type, were used to obtain a good signal-to-noise ratio and a higher spatial resolution in all studies retrieved. T1w, T2w, PDw, and TOF were used most frequently in 0.5–3 mm thickness for the basic evaluation of carotid plaque composition. Advanced sequences were used for the detection of specific plaque characteristics (eg, magnetization-prepared rapid gradient-echo [MPRAGE][15–20] or simultaneous non-contrast angiography and intraplaque hemorrhage [SNAP][18,21,22] containing 3D MPRAGE for detection of IPH) or complex plaque

15222586, 2025, 3, Downloaded from https://onlinelibrary.wiley.com/doi/10.1002/jmri.29522, Wiley Online Library on [04/09/2026]. See the Terms and Conditions (https://onlinelibrary.wiley.com/terms-and-conditions) on Wiley Online Library for rules of use; OA articles are governed by the applicable Creative Commons License

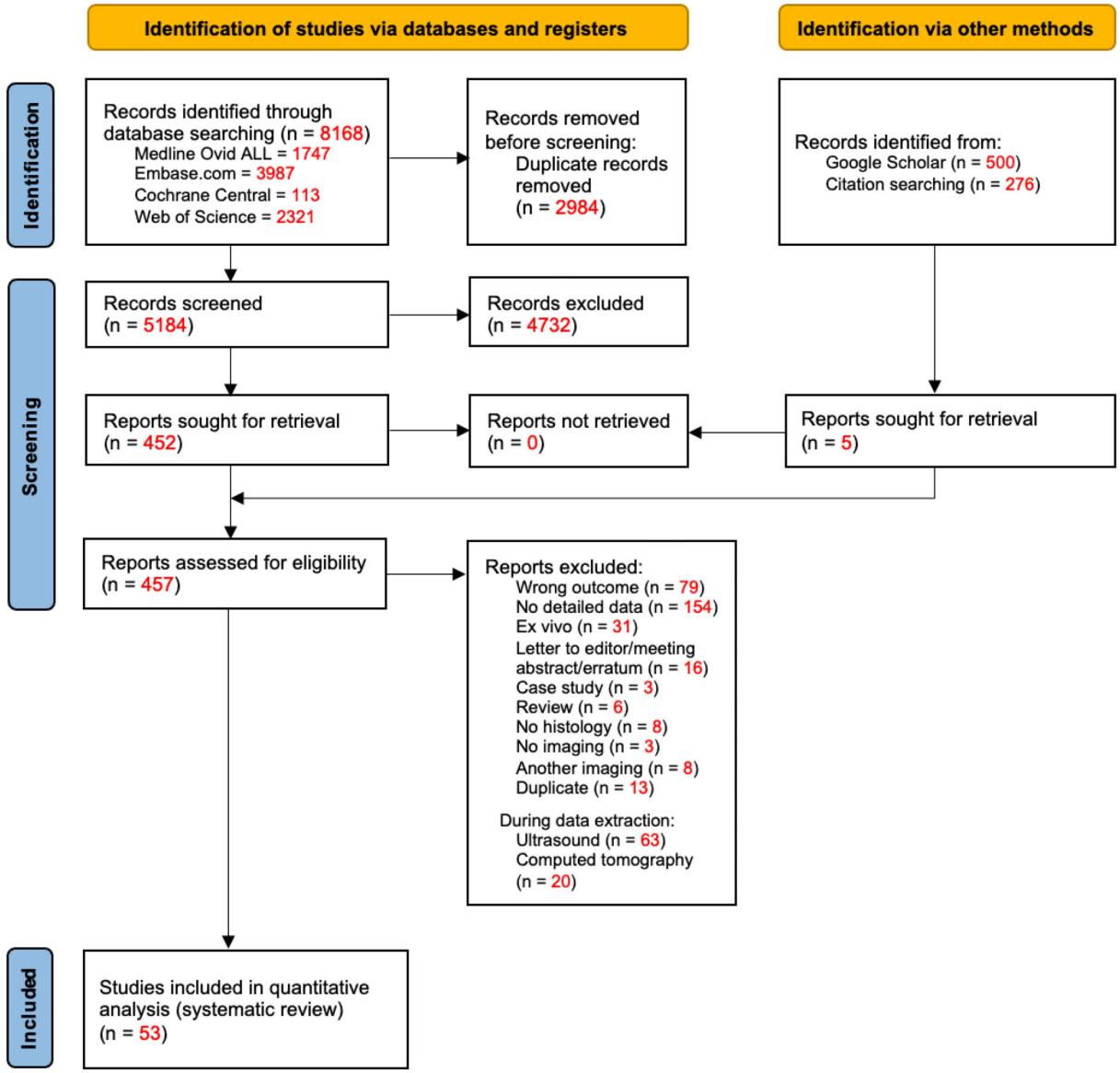


FIGURE 1: PRISMA[11] flow diagram of study selection.

structure (eg, multi-contrast atherosclerosis characterization [MATCH][17,23]). Besides the standard signal intensity measurement, tools for quantification of tissue alternations voxel by voxel were used, such as diffusion-weighted imaging (DWI),[24] T1w mapping (eg, SNAP with 3D golden angle radial k-space sampling [GOAL-SNAP][22]) or T2w mapping (eg, delay alternating with nutation for tailored excitation multi-echo spin echo [DANTE-MESE][25]). For imaging of blood flow in the stenotic part of the carotid artery, various magnetic resonance angiography techniques such as TOF (2D SNAP, 3D, or multiple overlapping thin slab angiography [MOTSA][26]) or contrast-enhanced angiography were used. Detailed information on the technical setting of all sequences used in retrieved studies is provided in Table S1 in the Supplemental Material.

Contrast-Enhanced Examinations

33% of all included studies (18/54) used contrast agent (CA) for contrast-enhanced MRI (CE-MRI) to detect specific carotid plaque characteristics, mainly inflammation, neovascularization, IPH, LRNC, ulceration, and fibrous cap. Only one study[24] used CA based on superparamagnetic particles of iron oxide (SPIO) usually used to detect liver tumors, among the rest used CA based on gadolinium. Precisely, gadolinium diethylenetriamine pentaacetic acid (Gd-DTPA),[19,28–34] gadopentetate dimeglumine,[6,35,36] gadobenate dimeglumine,[37] gadopentetate glucosamine,[38] gadodiamide,[36,39,40] and nonspecified Gd CA[41,42] were used. The dose of Gd CA given to the patients was 0.1–0.2 mmol/kg administered at a speed of 2–3 mL/s. All details on CA used in CE-MRI studies are provided in Table S2 in the Supplemental Material.

15222586, 2025, 3, Downloaded from https://onlinelibrary.wiley.com/doi/10.1002/jmri.29522, Wiley Online Library on [04/09/2026]. See the Terms and Conditions (https://onlinelibrary.wiley.com/terms-and-conditions) on Wiley Online Library for rules of use; OA articles are governed by the applicable Creative Commons License

Diagnostic Accuracy and Specific Plaque Characteristics

INTRAPLAQUE HEMORRHAGE. For the most common plaque characteristic investigated in the retrieved studies, 29 comparisons were found in 1.5 T MRI and 31 comparisons in 3 T MRI. Among all sequences, MPRAGE (3D T1w GRE) was used primarily to identify the presence of methemoglobin in the extracellular matrix,[15] where IPH shows a hyperintense signal, followed by multi-contrast MRI. Furthermore, multi-contrast MRI (T1w, T2w, PDw, TOF) can stage IPH in fresh (<1 week), recent (1–6 weeks), and old (>6 weeks) based on red blood cell content and hemoglobin oxygenation.[34,43] Imaging parameters for IPH were uniform in the retrieved studies (Table 1). 1.5 T machines showed a higher sensitivity 66.67%–100% (mean 86%) and specificity 53.33%–100% for IPH detection compared to 3 T machines, which showed a sensitivity 35.05%–100% and specificity 66.67%–100%. The 3D T1w sequence was found to be more accurate than 2D T1w,[44] but T1w 2D-CSE (chemical shift-encoded MRI) proved to be the most accurate in direct comparison with T1w 2D-FSE (fast spin echo) and T1w 3D-FSE.[45] The hyperintense signal on TOF[41] and T1w 2D-CSE[45] showed the highest sensitivity and specificity (both 100%). Regarding the area of IPH, larger areas (>2 mm^2) were detected by 1.5 T MRI with higher accuracy compared to all areas.[46] On 3 T MRI, the SNAP sequence uses phase-sensitive detection of IPH by generating three sets of images (IPH—strong positive signal, carotid lumen—strong negative signal, other tissue—near zero signal).[21] However, SNAP imaging showed mainly only good sensitivity 61%–85% with excellent specificity 88%–96%.[18,21] Compared to MPRAGE on 3 T MRI, SNAP[18] showed higher sensitivity and specificity, and MATCH showed higher sensitivity with the same specificity.[17] The T2 mapping technique[25] showed much better accuracy compared to the T1 mapping[22] and in direct comparison of CE-MRI with non-contrast TOF, CE-MRI proved to be more accurate. Detailed information on studies, sequences, and diagnostic accuracy of IPH can be found in Table 1.

LIPID-RICH NECROTIC CORE. Thirty-five comparisons of diagnostic accuracy were found for the detection of LRNC (23 on 1.5 T MRI; 12 on 3 T MRI). Sensitivity and specificity were found to be 61.54%–100% (mean 89%) and 40%–100% (mean 79%) for 1.5 T, respectively; and only 22.22%–86.67% (mean 66%) and 48.1%–100% (mean 78%) for 3 T, respectively. A single sequence (3D T1w) with a cutoff score of 180 was found to be the most accurate (sensitivity 92%, specificity 87%) compared to other scores and multi-sequence imaging.[47] However, LRNC identification as hyper/isointense (T1w/TOF) and hypo/isointense (PDw/T2w) were mainly used in all retrieved studies and found to be the most accurate on multi-sequence 1.5 T MRI (sensitivity 97.78%–100% and specificity 92.86%–100%).[48,49] Contrarily, 3 T showed mostly limited sensitivity and good specificity. T1 mapping[22] showed low accuracy, however, T2w mapping[25] showed similar good accuracy compared to MATCH[23] and compressed sensing motion-sensitizing driven equilibrium rapid gradient echo (CS-3DMERGE)[28] sequence. CE-MRI did not positively affect the accuracy.[19,30,31,33,42] Detailed information on LRNC is shown in Table 2.

CALCIFICATION. Calcification was investigated in seven 1.5 T MRI comparisons and revealed a high and consistent sensitivity 76.42%–85.71% (mean 81%) and specificity 85.71%–100% (mean 91%). Six 3 T MRI comparisons resulted in a sensitivity 81.25%–100% (mean 92%) and a specificity of 75%–100% (mean 90%). The MRI definitions of calcification were uniform in the retrieved studies. Multi-contrast imaging showing calcification as hypointense on all sequences proved to be the most accurate. In 3 T, the T2 mapping (DANTE-MESE) showed perfect sensitivity and specificity (both 100%),[25] the same as the CS-3DMERGE sequence.[28] The studies that investigated calcification are shown in Table 3.

FIBROUS PLAQUE. Seven comparisons were found in the detection of fibrous plaque, including two in 3 T MRI. The 3 T studies showed better sensitivity (75%–100%) and lower specificity (79%–95.45%) compared to the 1.5 studies (50%–78.5% and 83.3%–100%, respectively). The MRI definitions of fibrous plaque were not uniform as shown in Table 4. The T2 mapping (3 T MRI) showed the most accurate results (sensitivity 100%, specificity 95.45%).

FIBROUS CAP. The accuracy of fibrous cap detection was investigated in nine comparisons (three on 3 T MRI), all listed in Table 5. Sensitivity 75%–100% (mean 89%; 80.65%–100% for ruptured fibrous cap) and specificity 68.75%–100% (mean 87%; 68.75%–96.3% for ruptured fibrous cap) were found in 1.5 T, and specificity 69%–90% and specificity 82%–85% for ruptured fibrous cap in 3 T. Uniform evaluation as a hypointense band on TOF and CE-MRI showed all studies. 3D MOTSA[26] on 1.5 T and CE-MRI[38] on 3 T showed the highest accuracy. CE-MRI showed better performance in detecting plaque rupture with higher sensitivity (90%) and specificity (83.3%) than digital subtraction angiography (DSA; 40% and 66.7%, respectively).[38]

ULCERATION. Surface ulceration of carotid plaque and MRI accuracy were tested in 11 studies (a single study on 3 T MRI with moderate accuracy[42]; Table 6). Ulceration was defined uniformly as surface disruption (usually ulcers with depth >1 mm). The 1.5 T MRI detected ulceration with

15222586, 2025, 3, Downloaded from https://onlinelibrary.wiley.com/doi/10.1002/jmri.29522, Wiley Online Library on [04/09/2026]. See the Terms and Conditions (https://onlinelibrary.wiley.com/terms-and-conditions) on Wiley Online Library for rules of use; OA articles are governed by the applicable Creative Commons License

TABLE 1. Diagnostic Accuracy of MRI in Detection of Intraplaque Hemorrhage

First Author	Specific Sequences	Number of Patients	Number in Analysis	Plaque Characteristic (MRI)	Plaque Characteristic (Histology)	Sensitivity (%)	Specificity (%)
Intraplaque hemorrhage—1.5 Tesla							
Albuquaerque 2007[15]	MPRAGE	70	70	Hyperintense signal	Acute/recent hemorrhage by Lusby	95.65	95.83
Altaf 2013[16]	MPRAGE	35	35	Plaque hemorrhage^{+}	AHA plaque type VI	79.17	81.82
Bitar 2008[82]	T1w	11	194	Hyperintense signal	Hemorrhage	96.77	84.09
Cai 2002a[51]	T1w; TOF	60	252	High signal intensity	AHA plaque type VI	81.52	91.25
Cappendijk 2004a[44]	3D T1w	11	188	High signal intensity	Hemorrhage	87.21	84.31
Cappendijk 2004b[44]	2D T1w	11	188	High signal intensity	Hemorrhage	81.40	56.86
Chu 2004a[43]	T1w, PDw, T2w, TOF	27	378	Hemorrhage	Hemorrhage	90.00	73.86
Chu 2004b[43]	T1w, PDw, T2w, TOF	27	378	Hyperintense (T1w/TOF), hypo/isointense (T2w/PDw)	Fresh hemorrhage	52.17	98.87
Chu 2004c[43]	T1w, PDw, T2w, TOF	27	378	Hyperintense on all sequences	Recent hemorrhage	83.41	94.01
Chu 2004d[43]	T1w, PDw, T2w, TOF	27	378	Hypointense on all sequences	Old hemorrhage	76.47	92.44
Esposito 2007a[48]	T1w, PDw, T2w, TOF	77	21	High signal intensity on all sequences	AHA plaque type VI	66.67	94.44
Honda 2006a[50]	TOF	17	18	High signal intensity	Hemorrhage	80.00	100
Ideguchi 2009a[41]	TOF	8	8	High signal	Hemorrhage	100	100
Kampschulte 2004a[83]	TOF, T1w, T2w, PDw	24	190	Characteristic signal intensities (multicontrast), deep within the plaque, juxtaluminal band of low signal intensity	Intraplaque hemorrhage with thick fibrous cap	93.00	86.67

15222586, 2025, 3, Downloaded from https://onlinelibrary.wiley.com/doi/10.1002/jmri.29522, Wiley Online Library on [04/09/2026]. See the Terms and Conditions (https://onlinelibrary.wiley.com/terms-and-conditions) on Wiley Online Library for rules of use; OA articles are governed by the applicable Creative Commons License

TABLE 1. Continued

First Author	Specific Sequences	Number of Patients	Number in Analysis	Plaque Characteristic (MRI)	Plaque Characteristic (Histology)	Sensitivity (%)	Specificity (%)
Kampschulte 2004b[83]	TOF, T1w, T2w, PDw	24	190	Characteristic signal intensities (multicontrast), lumen adjacent and absent dark juxtaluminal band of signal intensity (TOF)	Juxtaluminal hemorrhage/thrombus	87.50	98.00
Lukanova 2015a[6]	T1w, T2w/PDw, CE-MRI	25	30	AHA type VI for MRI	Hemorrhage	92.31	94.12
Narumi 2017a[45]	T1w 2D-CSE	35	35	AHA type VI for MRI	AHA type VI	100	100
Narumi 2017b[45]	T1w 2D-FSE	35	35	AHA type VI for MRI	AHA type VI	94.10	100
Narumi 2017c[45]	T1w 3D-FSE	35	35	AHA type VI for MRI	AHA type VI	100	94.40
Puppini 2006a[86]	TOF, T1w, T2w, PDw	15	56	Hyperintense (TOF), hyper-isointense (T1w), hypo-isointense (T2w/PDw)	Hemorrhage	91.67	100
Saam 2005a[46]	T1w, T2w, PDw, TOF	31	214	Hyperintense (T1w/TOF), hyper/isointense (T2w/PD)	Hemorrhage (all areas)	82.28	77.27
Saam 2005b[46]	T1w, T2w, PDw, TOF	31	214	Hyperintense (T1w/TOF), hyper/isointense (T2w/PD)	Hemorrhage (areas >2 mm^2)	87.02	84.34
Saito 2013a[84]	T1w	25	25	High signal	Large hemorrhage	90.00	53.33
Saito 2013b[84]	T1w, TOF	25	25	High signal (T1w); iso-signal (TOF)	Large hemorrhage	70.00	100
Yim 2008a[34]	T1w, T1w FS, T2w, PDw, TOF, CE-MRI	135	135	High signal intensity (T1w FS/TOF), low signal intensity (T2w)	Hemorrhage	90.48	83.87
Yim 2008b[34]	TOF	135	135	High signal intensity halo sign (MIP images)	Hemorrhage	92.86	84.95

15222586, 2025, 3, Downloaded from https://onlinelibrary.wiley.com/doi/10.1002/jmri.29522, Wiley Online Library on [04/09/2026]. See the Terms and Conditions (https://onlinelibrary.wiley.com/terms-and-conditions) on Wiley Online Library for rules of use; OA articles are governed by the applicable Creative Commons License

TABLE 1. Continued

First Author	Specific Sequences	Number of Patients	Number in Analysis	Plaque Characteristic (MRI)	Plaque Characteristic (Histology)	Sensitivity (%)	Specificity (%)
Yim 2008c[34]	T1w, T1w FS, T2w, PDw, TOF, CE-MRI	42	42	High signal intensity (T1w/TOF), iso- to low signal intensity (T2w)	Fresh hemorrhage	80.00	85.19
Yim 2008d[34]	T1w, T1w FS, T2w, PDw, TOF, CE-MRI	42	42	High signal intensity on all contrast-weighted sequences	Recent hemorrhage	90.91	65.00
Yim 2008e[34]	T1w, T1w FS, T2w, PDw, TOF, CE-MRI	42	42	Low signal intensity on all contrast-weighted sequences	Old hemorrhage	–	90.48
Intraplaque hemorrhage—3.0 Tesla							
Chai 2017a[25]	T2w mapping DANTE-MESE	26	26	Thresholds value T2 > T2H; >5% of the total cross-sect. area	AHA plaque type VI	87.50	88.89
Dai 2017a[23]	MATCH	46	298	Hyper-T1w: hyperintense; T2w: hyper- or isointense	Hemorrhage	84.20	81.00
Dai 2017b[23]	T1w, T2w, PDw, TOF	46	298	Hyperintense	Hemorrhage	73.70	81.00
Dong 2017a[28]	CS-3D MERGE	21	21	Hyperintense	Hemorrhage	73.33	66.67
Du 2017a[17]	MATCH	30	95	Hyperintense (T1w)	Hemorrhage	93.15	90.91
Du 2017b[17]	MPRAGE	30	95	Hyperintense (2× higher to surrounding muscle)	Hemorrhage	87.67	90.91
Li D 2020a[18]	SNAP	35	128	Hyperintense (signal intensity ratio ≥1.5:1)	Hemorrhage	85.00	89.58
Li D 2020b[18]	MPRAGE	35	128	Hyperintense (signal intensity ratio ≥1.5:1)	Hemorrhage	75.00	79.17
Liu J 2019a[21]	SNAP	14	121	Artery wall max. normalized intensity (semiautomatic)	Hemorrhage	61.00	88.00

15222586, 2025, 3, Downloaded from https://onlinelibrary.wiley.com/doi/10.1002/jmri.29522, Wiley Online Library on [04/09/2026]. See the Terms and Conditions (https://onlinelibrary.wiley.com/terms-and-conditions) on Wiley Online Library for rules of use; OA articles are governed by the applicable Creative Commons License

TABLE 1. Continued

First Author	Specific Sequences	Number of Patients	Number in Analysis	Plaque Characteristic (MRI)	Plaque Characteristic (Histology)	Sensitivity (%)	Specificity (%)
Liu J 2019b[21]	SNAP	14	121	Artery wall max. normalized intensity (manual)	Hemorrhage	63.00	96.00
Liu W 2018[85]	T1w, T2w	10	236	High signal intensity	Hemorrhage	76.74	95.33
Millon 2012a[30]	TOF, T1w, PDw, CE-MRI	59	59	Hyper-signal on all sequences	Hemorrhage	72.22	97.56
Millon 2013a[31]	TOF, T1w, PDw, CE-MRI	79	79	Hyper-signal on all sequences	Hemorrhage	71.00	97.00
Ota 2018a[19]	T1w/T2w VISTA, TOF, MPRAGE, CE-MRI	12	21	Hemorrhage on probability density map (ADC and R1)	Hemorrhage	71.00	82.00
Ota 2010a[20]	T1w	20	231	High signal intensity	Hemorrhage	47.42	91.79
Ota 2010b[20]	T1w	20	195	High signal intensity	Hemorrhage (IPH areas <2.81 mm^2 excluded)	59.02	91.79
Ota 2010c[20]	T1w	20	184	High signal intensity	Hemorrhage (IPH areas <2.81 mm^2 heavily calcified IPHs excluded)	70.00	91.79
Ota 2010d[20]	TOF	20	231	High signal intensity	Hemorrhage	35.05	95.52
Ota 2010e[20]	TOF	20	195	High signal intensity	Hemorrhage (IPH areas <2.81 mm^2 excluded)	45.90	95.52
Ota 2010f[20]	TOF	20	184	High signal intensity	Hemorrhage (IPH areas <2.81 mm^2/heavily calcified IPHs excluded)	56.00	95.52
Ota 2010g[20]	MPRAGE	20	231	High signal intensity	Hemorrhage	47.42	97.01

15222586, 2025, 3, Downloaded from https://onlinelibrary.wiley.com/doi/10.1002/jmri.29522, Wiley Online Library on [04/09/2026]. See the Terms and Conditions (https://onlinelibrary.wiley.com/terms-and-conditions) on Wiley Online Library for rules of use; OA articles are governed by the applicable Creative Commons License

TABLE 1. Continued

First Author	Specific Sequences	Number of Patients	Number in Analysis	Plaque Characteristic (MRI)	Plaque Characteristic (Histology)	Sensitivity (%)	Specificity (%)
Ota 2010h[20]	MPRAGE	20	195	High signal intensity	Hemorrhage (IPH areas <2.81 mm^2 excluded)	65.57	97.01
Ota 2010i[20]	MPRAGE	20	184	High signal intensity	Hemorrhage (IPH areas <2.81 mm^2/heavily calcified IPHs excluded)	80.00	97.01
Qiao H 2020a[22]	3D T1w mapping GOAL-SNAP	19	52	Mean T1 value of hemorrhage	Hemorrhage	83.33	68.75
Qiao H 2020b[22]	3D T1w mapping GOAL-SNAP	19	30	Mean T1 value of fresh hemorrhage ≥50%	Fresh hemorrhage ≥50%	71.43	68.75
Qiao Y 2011a[36]	3D FFE + CE-MRI	15	144	Hyperintense signal intensity	Hemorrhage	87.30	98.77
Qiao Y 2011b[36]	3D TOF	15	144	Hyperintense signal intensity	Hemorrhage	79.37	87.04
Sigovan 2017a[32]	2D T1w	18	18	Hyper-intense signal	Hemorrhage	58.33	100
Sigovan 2017b[32]	3D T1w	18	18	Hyper-intense signal	Hemorrhage	100	83.33
Tapis 2020a[42]	TOF, T1w, T2w, CE-MRI	36	36	Hyperintense (TOF/T1w), hypo-/isointense (T2w/CE-T1w)	Hemorrhage	62.96	77.78
Wang Z 2019a[33]	T1w SPACE	28	28	Bright and high signal	Hemorrhage	90.00	75.00

MPRAGE = magnetization-prepared rapid gradient-echo; AHA = American Heart Association; TOF = time of flight; DIR = double inversion recovery; PD = proton dense; CE-MRI = contrast enhanced magnetic resonance imaging; ECG = electrocardiography; CSE = conventional spin echo; FSE = fast spin echo; FS = fat saturation; DANTE = delay alternating with nutation for tailored excitation; MESE = multiecho spin echo; CS-3D MERGE = compressed sensing three dimensional motion-sensitized driven equilibrium prepared rapid gradient echo; SNAP = simultaneous non-contrast angiography and intraplaque hemorrhage; VISTA = volume isotropic acquisition; IPH = intraplaque hemorrhage; GOAL = 3D golden angle radial k-space sampling; FFE = fast field echo; SPACE = sampling perfection with application optimized contrast using different flip angle evolution.

15222586, 2025, 3, Downloaded from https://onlinelibrary.wiley.com/doi/10.1002/jmri.29522, Wiley Online Library on [04/09/2026]. See the Terms and Conditions (https://onlinelibrary.wiley.com/terms-and-conditions) on Wiley Online Library for rules of use; OA articles are governed by the applicable Creative Commons License

TABLE 2. Diagnostic Accuracy of MRI in Detection of Lipid-Rich Necrotic Core

First Author	Specific Sequences	Number of Patients	Number in Analysis	Plaque Characteristic (MRI)	Plaque Characteristic (Histology)	Sensitivity (%)	Specificity (%)
Lipid-rich necrotic core—1.5 Tesla							
Cai 2002b[51]	T1w; PDw; T2w	60	252	High-/isosignal (T1w/PDw), varied signal (T2w)	AHA plaque type IV-V	83.93	90.31
Cappendijk 2008a[47]	Multiseq (3D T1w; T2w, PDw, T1w, part-T2w)	64	327	Lipid core (cutoff score 0)	Lipid core	84.00	71.00
Cappendijk 2008b[47]	Multiseq (3D T1w; T2w, PDw, T1w, part-T2w)	64	327	Lipid core (cutoff score 90)	Lipid core	82.00	86.00
Cappendijk 2008c[47]	Multiseq (3D T1w; T2w, PDw, T1w, part-T2w)	64	327	Lipid core (cutoff score 180)	Lipid core	92.00	81.00
Cappendijk 2008d[47]	Multiseq (3D T1w; T2w, PDw, T1w, part-T2w)	64	327	Lipid core (cutoff score 270)	Lipid core	100	77.00
Cappendijk 2008e[47]	Multiseq (3D T1w; T2w, PDw, T1w, part-T2w)	64	327	Lipid core (cutoff score 360)	Lipid core	100	69.00
Cappendijk 2008f[47]	Single (3D T1w)	64	327	Lipid core (cutoff score 0)	Lipid core	77.00	71.00
Cappendijk 2008g[47]	Single (3D T1w)	64	327	Lipid core (cutoff score 90)	Lipid core	86.00	87.00
Cappendijk 2008h[47]	Single s (3D T1w)	64	327	Lipid core (cutoff score 180)	Lipid core	92.00	87.00
Cappendijk 2008i[47]	Single (3D T1w)	64	327	Lipid core (cutoff score 270)	Lipid core	100	81.00
Cappendijk 2008j[47]	Single (3D T1w)	64	327	Lipid core (cutoff score 360)	Lipid core	100	77.00
Esposito 2007b[48]	TOF, T1w, T2w, PDw	77	21	TOF/T1w: isointense; PDw/T2w: iso/hyperintense	AHA plaque type IV-V	100	92.86

15222586, 2025, 3, Downloaded from https://onlinelibrary.wiley.com/doi/10.1002/jmri.29522, Wiley Online Library on [04/09/2026]. See the Terms and Conditions (https://onlinelibrary.wiley.com/terms-and-conditions) on Wiley Online Library for rules of use; OA articles are governed by the applicable Creative Commons License

TABLE 2. Continued

First Author	Specific Sequences	Number of Patients	Number in Analysis	Plaque Characteristic (MRI)	Plaque Characteristic (Histology)	Sensitivity (%)	Specificity (%)
Ideguchi 2009b[41]	T1w	8	8	High signal	Lipid-rich necrotic core	100	66.67
Kawahara 2007a[35]	T1w	9	10	High signal intensity	Lipid-rich plaque (AHA Va-VI)	85.71	100
Lukanova 2015b[6]	T1w, T2w/PDw, CE-MRI	25	30	AHA type IV-V for MRI	Lipid content >30%	92.86	93.75
Puppini 2006b[86]	TOF, T1w, T2w, PDw	15	56	Hyperintense (T1w), isointense (TOF), variable (T2w/PDw)	Lipid core	91.67	95.00
Saam 2005c[46]	T1w, T2w, PDw, TOF	31	214	Iso/hyperintense: T1w/PDw, varied: T2w/TOF	Lipid/necrotic core (all areas)	92.12	65.31
Saam 2005d[46]	T1w, T2w, PDw, TOF	31	214	Iso/hyperintense: T1w/PDw, varied: T2w/TOF	Lipid/necrotic core (areas >2 mm^2)	95.14	75.71
Saito 2013c[84]	T1w	25	25	High signal	Lipid-rich plaque	76.92	50.00
Saito 2013d[84]	T1w, TOF	25	25	T1w: high signal; TOF: iso-signal	Lipid-rich plaque	61.54	91.67
Takemoto 2013a[87]	T1w	69	71	Plaque/muscle ratio cut-off 1.51>	Atheroma-predominant plaque (>50%; Type Va1)	75.00	73.00
Young 2010[24]	TOF, T1w, T2w, PDw, DWI	19	19	Hypointense, low ADC values	Lipid-rich necrotic core	85.71	40.00
Yuan 2001a[49]	T1w, T2w, PDw, TOF	18	90	Hyperintense (T1w), hypo/isointense (PDw/T2w), isointense (TOF)	Lipid core	97.78	100
Lipid-rich necrotic core—3.0 Tesla							
Chai 2017b[25]	T2w mapping DANTE-MESE	26	26	Voxels with T2 <42 msec or T2 >90 msec	AHA plaque type IV-V	77.78	88.24
Dai 2017c[23]	MATCH	46	298	T2w: hypointense; hyper-T1w: isointense	Lipid core	84.20	81.00
Dai 2017d[23]	T1w, T2w, PDw, TOF	46	298	T1w/PDw: iso/hyperintense; T2w/TOF: hypo/isointense	Lipid core	77.30	83.30

15222586, 2025, 3, Downloaded from https://onlinelibrary.wiley.com/doi/10.1002/jmri.29522, Wiley Online Library on [04/09/2026]. See the Terms and Conditions (https://onlinelibrary.wiley.com/terms-and-conditions) on Wiley Online Library for rules of use; OA articles are governed by the applicable Creative Commons License

TABLE 2. Continued

First Author	Specific Sequences	Number of Patients	Number in Analysis	Plaque Characteristic (MRI)	Plaque Characteristic (Histology)	Sensitivity (%)	Specificity (%)
Dong 2017b[28]	CS-3DMERGE	21	21	Isointense	Lipid core	86.67	50.00
Millon 2012b[30]	TOF, T1w, PDw, CE-MRI	59	59	Iso-signal (TOF/T1w); hypo/iso-signal (PDw)	Large lipid core >50%	67.74	75.00
Millon 2013b[31]	TOF, T1w, PDw, CE-MRI	79	79	Isosignal (PDw/T1w); hyposignal (CE-T1w)	Large lipid core >50%	70.00	78.00
Ota 2018b[19]	T1w/T2w VISTA, TOF, MPRAGE, CE-MRI	12	21	LRNC on probability density map (ADC and R1)	Lipid/necrotic core	60.00	93.00
Qiao H 2020c[22]	3D T1w mapping GOAL-SNAP	19	52	Mean T1 value of necrotic core	Necrotic core	60.00	48.10
Tapis 2020b[42]	TOF, T1w, T2w, CE-MRI	36	36	Isointense (TOF), hyperintense (T1w), variable intensity (T2w), hypointense (CE-MRI)	Lipid-rich necrotic core (total)	59.38	100
Tapis 2020c[42]	TOF, T1w, T2w, CE-MRI	36	36	Isointense (TOF), hyperintense (T1w), variable intensity (T2w), hypointense (CE-MRI)	Lipid-rich necrotic core (large)	42.86	77.27
Tapis 2020d[42]	TOF, T1w, T2w, CE-MRI	36	36	Isointense (TOF), hyperintense (T1w), variable intensity (T2w), hypointense (CE-MRI)	Lipid-rich necrotic core (small)	22.22	77.78
Wang Z 2019b[33]	T1w SPACE	28	28	Isointense, nonenhanced (CE-MRI)	Lipid-rich necrotic core	83.33	80.00

PD = proton dense; AHA = American Heart Association; TOF = time of flight; CE-MRI = contrast enhanced magnetic resonance imaging; ADC = apparent diffusion coefficient; DWI = diffusion weighted imaging; DANTE = delay alternating with nutation for tailored excitation; MESE = multiecho spin echo; CS-3D MERGE = compressed sensing three dimensional motion-sensitized driven equilibrium prepared rapid gradient echo; MATCH = multicontrast atherosclerosis characterization; VISTA = volume isotropic acquisition; MPRAGE = magnetization prepared rapid gradient echo; GOAL-SNAP = simultaneous noncontrast angiography and intraplaque hemorrhage imaging with 3D golden angle radial k-space sampling; SPACE = sampling perfection with application optimized contrast using different flip angle evolution.

15222586, 2025, 3, Downloaded from https://onlinelibrary.wiley.com/doi/10.1002/jmri.29522, Wiley Online Library on [04/09/2026]. See the Terms and Conditions (https://onlinelibrary.wiley.com/terms-and-conditions) on Wiley Online Library for rules of use; OA articles are governed by the applicable Creative Commons License

TABLE 3. Diagnostic Accuracy of MRI in Detection of Calcification, Fibrous Cap, and Plaque Surface

First Author	Specific Sequences	Number of Patients	Number in Analysis	Plaque Characteristic (MRI)	Plaque Characteristic (Histology)	Sensitivity (%)	Specificity (%)
Calcification—1.5 Tesla							
Cai 2002c[51]	T1w; PDw; T2w; TOF	60	252	Irregular low signal intensity on all sequences	AHA plaque type VII	80.43	93.98
Esposito 2007c[48]	TOF, T1w, T2w, PDw	77	21	Low signal intensity on all sequences	AHA plaque type VII	85.71	100
Puppini 2006c[86]	TOF, T1w, T2w, PDw	15	56	Hypointense on all sequences	Calcification	80.00	93.75
Saam 2005e[46]	T1w, T2w, PDw, TOF	31	214	Hypointense on all sequences	Calcification (all areas)	76.42	85.71
Saam 2005f[46]	T1w, T2w, PDw, TOF	31	214	Hypointense on all sequences	Calcification (areas >2 mm^2)	83.51	91.45
Takemoto 2013b[87]	T1w	69	71	Plaque/muscle ratio cut-off 1.18<	Predominant calcification with a fibrolipid lesion (Type Vb)	81.00	87.50
Takemoto 2013c[87]	T2w	69	71	Plaque/muscle ratio cut-off 1.81<	Predominant calcification with a fibrolipid lesion (Type Vb)	81.00	87.50
Calcification—3.0 Tesla							
Chai 2017c[25]	T2w mapping DANTE-MESE	26	26	Calcification (AHA—VII)	AHA plaque type VII	100	100
Dai 2017e[23]	MATCH	46	298	Hypointense on gray-blood images	Calcification	100	81.80
Dai 2017f[23]	T1w, T2w, PDw, TOF	46	298	Hypointense on all sequences	Calcification	82.40	82.60
Dong 2017c[28]	CS-3DMERGE	21	21	No signal	Calcification	100	100
Tapis 2020e[42]	TOF, T1w, T2w, CE-MRI	36	36	Hypointense in all sequences	Calcification	81.25	75.00
Wang Z 2019c[33]	T1w SPACE	28	28	Very low signal	Calcification	91.30	100

PD = proton dense; AHA = American Heart Association; TOF = time of flight; CE-MRI = contrast enhanced magnetic resonance imaging; DANTE = delay alternating with nutation for tailored excitation; MESE = multiecho spin echo; CS-3DMERGE = compressed sensing three dimensional motion-sensitized driven equilibrium prepared rapid gradient echo; MATCH = multicontrast atherosclerosis characterization; SPACE = sampling perfection with application optimized contrast using different flip angle evolution.

15222586, 2025, 3, Downloaded from https://onlinelibrary.wiley.com/doi/10.1002/jmri.29522, Wiley Online Library on [04/09/2026]. See the Terms and Conditions (https://onlinelibrary.wiley.com/terms-and-conditions) on Wiley Online Library for rules of use; OA articles are governed by the applicable Creative Commons License

TABLE 4. Diagnostic Accuracy of MRI in Detection of Fibrous Plaque

First Author	Specific Sequences	Number of Patients	Number in Analysis	Plaque Characteristic (MRI)	Plaque Characteristic (Histology)	Sensitivity (%)	Specificity (%)
Fibrous plaque—1.5 Tesla							
Cai 2002d[51]	T1w; PDw; T2w; TOF	60	252	Highly fibrotic lesion (AHA types IV-V to VII excluded)	AHA plaque type VIII	55.56	100
Esposito 2007d[48]	TOF, T1w, T2w, PDw	77	21	Iso- to slightly high-intense on all sequences	AHA plaque type VIII	–	90.48
Honda 2007[88]	TOF, T1w, T2w, PDw	6	7	Fibrous plaque	Fibrous plaque	50.00	100
Ideguchi 2009c[41]	T1w	8	8	Low to equal signal	Fibrous plaque	66.67	100
Takemoto 2013d[87]	T1w	69	71	Plaque/muscle ratio cut-off 1.18<	Connective tissue-predominant plaque (Type Va2)	78.50	83.30
Fibrous plaque—3.0 Tesla							
Chai 2017d[25]	T2w mapping DANTE-MESE	26	26	Fibrous part (AHA—VIII)	AHA plaque type VIII	100	95.45
Ota 2018c[19]	T1w/T2w VISTA, TOF, MPRAGE, CE-MRI	12	21	Fibrous part on probability density map (ADC and R1)	Fibrous part	75.00	79.00

PD = proton dense; AHA = American Heart Association; TOF = time of flight; CE-MRI = contrast enhanced magnetic resonance imaging; ADC = apparent diffusion coefficient; DANTE = delay alternating with nutation for tailored excitation; MESE = multiecho spin echo; MOTSA = multiple overlapping thin slab angiography; VISTA = volume isotropic acquisition; MPRAGE = magnetization prepared rapid gradient echo.

15222586, 2025, 3, Downloaded from https://onlinelibrary.wiley.com/doi/10.1002/jmri.29522, Wiley Online Library on [04/09/2026]. See the Terms and Conditions (https://onlinelibrary.wiley.com/terms-and-conditions) on Wiley Online Library for rules of use; OA articles are governed by the applicable Creative Commons License

TABLE 5. Diagnostic Accuracy of MRI in Detection of Fibrous Cap

First Author	Specific Sequences	Number of Patients	Number in Analysis	Plaque Characteristic (MRI)	Plaque Characteristic (Histology)	Sensitivity (%)	Specificity (%)
Fibrous cap—1.5 Tesla							
Hatsukami 2000a[26]	3D MOTSA	19	36	Dark band between white lumen/gray wall	Intact thick fibrose cap	100	87.50
Hatsukami 2000b[26]	3D MOTSA	19	36	No band between white lumen/gray wall	Intact thin fibrose cap	75.00	100
Hatsukami 2000c[26]	3D MOTSA	19	36	No band between white lumen/gray wall, bright gray region near lumen	Ruptured fibrose cap	88.89	96.30
Mitsumori 2003[89]	TOF, T1w, PDw, T2w	18	91	Interrupted/irregular juxtaluminal hypointense band (TOF); absence of intimal tissue between lumen/deeper structures; focal luminal surface contour abnormalities	Unstable fibrous cap	80.65	90.00
Puppini 2006d[86]	TOF, T1w, T2w, PDw	15	23	Lack of the hypointense band (TOF)	Disrupted fibrous cap	100	80.00
Watanabe 2014[90]	TOF, T1w, T2w	35	97	Lack of the hypointense band (TOF)	Fibrous cap rupture	89.80	68.75
Fibrous cap—3.0 Tesla							
Millon 2012c[30]	TOF, T1w, PDw, CE-MRI	59	59	Disrupted dark band/no visible dark band lumen adjacent (TOF); cap discontinuity (CE-MRI)	Ruptured fibrose cap	69.00	85.00
Millon 2013c[31]	TOF, T1w, PDw, CE-MRI	79	79	Fibrous cap discontinuity	Ruptured fibrose cap	70.00	82.00
Wang Q 2011[38]	CE-MRI	21	22	Enhanced linear shadow continuity disruption	Plaque rupture	90.00	83.33

PD = proton dense; TOF = time of flight; CE-MRI = contrast enhanced magnetic resonance imaging; MOTSA = multiple overlapping thin slab angiography.

15222586, 2025, 3, Downloaded from https://onlinelibrary.wiley.com/doi/10.1002/jmri.29522, Wiley Online Library on [04/09/2026]. See the Terms and Conditions (https://onlinelibrary.wiley.com/terms-and-conditions) on Wiley Online Library for rules of use; OA articles are governed by the applicable Creative Commons License

TABLE 6. Diagnostic Accuracy of MRI in Detection of Ulceration

First author	Specific Sequences	Number of Patients	Number in Analysis	Plaque Characteristic (MRI)	Plaque Characteristic (Histology)	Sensitivity (%)	Specificity (%)
Ulceration—1.5 Tesla							
D'Onofrio 2006[29]	CE-MRI	21	41	Ulceration	Ulceration	71.00	100
Honda 2006b[50]	TOF, PDw, T2w, T1w	17	18	Ulceration	Ulceration	100	100
Ideguchi 2009d[41]	TOF	8	8	Ulceration	Ulceration	80.00	100
Ideguchi 2009e[41]	CE-MRI	8	8	Ulceration	Ulceration	100	100
Liberopoulos 1996[14]	TOF	52	63	Ulceration	Ulceration	90.70	–
Lukanova 2015c[6]	T1w, T2w/PDw, CE-MRI	25	30	Ulceration	Ulceration (ruptured fibrous cap)	77.78	90.48
Yu 2009a[39]	Cross sectional (T1w, T2w, PDw, TOF, CE-MRI)	32	38	Surface disruption with a depression into the plaque containing a disorganized blood flow signal on all sequences	Ulceration (all ulcers)	23.81	88.24
Yu 2009b[39]	Cross sectional (T1w, T2w, PDw, TOF, CE-MRI)	32	38	Surface disruption with a depression into the plaque containing a disorganized blood flow signal on all sequences	Ulceration (at least 6 mm^3)	30.00	67.86
Yu 2009c[39]	Cross sectional (T1w, T2w, PDw, TOF, CE-MRI) + 2D BB TOF	32	38	Surface disruption with a depression into the plaque containing a disorganized blood flow signal on all sequences	Ulceration (all ulcers)	52.38	82.35
Yu 2009d[39]	Cross sectional (T1w, T2w, PDw, TOF, CE-MRI) + 2D BB TOF	32	38	Surface disruption with a depression into the plaque containing a disorganized blood flow signal on all sequences	Ulceration (at least 6 mm^3)	80.00	64.29
Ulceration—3.0 Tesla							
Tapis 2020f[42]	TOF, T1w, T2w, CE-MRI	36	36	Ulceration	Ulceration	50.00	53.85

PD = proton dense; TOF = time of flight; CE-MRI = contrast enhanced magnetic resonance imaging; BB = black blood.

15222586, 2025, 3, Downloaded from https://onlinelibrary.wiley.com/doi/10.1002/jmri.29522, Wiley Online Library on [04/09/2026]. See the Terms and Conditions (https://onlinelibrary.wiley.com/terms-and-conditions) on Wiley Online Library for rules of use; OA articles are governed by the applicable Creative Commons License

sensitivity 23.81%–100% (mean 71%) and specificity 64.29%–100% (mean 88%). TOF and CE-MRI[41] were found to be the most accurate (accuracy 100%).

NEOVASCULARIZATION. Two 1.5 T and one 3 T studies investigated neovascularization (Table 7). All studies used CE-MRI with a uniform definition of neovascularization within the plaque (contrast enhancement) and 1.5 T studies[35,40] showed better sensitivity and specificity (76%–85.71% and 79.2%–100%, respectively) compared to the 3 T study[30] (sensitivity 77.78%, specificity 69.57%).

INFLAMMATION. Three studies showed diagnostic accuracy for plaque inflammation, including one in 3 T (Table 8). All studies used CE-MRI and the same definition (plaque contrast enhancement). Although one study[27] used SPIO for CE-MRI and reached a sensitivity of 62.5% and 100% specificity, Gd-based CA in the second study[37] revealed a better sensitivity (77.78%) and a lower specificity (84.62%). The 3 T study[30] showed similar sensitivity (69.5%) but significantly lower specificity (60%).

LOOSE MATRIX. Four comparisons in 3 T MRI and two comparisons in 1.5 T MRI were found for the detection of carotid plaque loose matrix (Table 9). A similar MR definition of the plaque characteristic was used in all studies (hyperintense: T2w/PDw, iso/hyperintense: T1w, isointense: TOF). Larger areas were detected with better accuracy (sensitivity 78.79%, specificity 77.03%) on 1.5 T MRI,[46] but 3 T MRI showed better results, mostly in terms of sensitivity (79.2%–90.9%; specificity 42.9%–93.1%). Although T1w mapping showed the lowest specificity (42.9%),[22] multisequence imaging showed the most accurate results (sensitivity 81.8%, specificity 93.1%), when also compared to the MATCH sequence in the same study.[23]

UNSTABLE PLAQUE. The diagnostic accuracy of unstable or soft or vulnerable plaque (by authors' definition mentioned in retrieved studies) was assessed in 19 comparisons (two 3 T MRI comparisons with sensitivity 79.49%–80% and specificity 55.88%–80% included).[30] A range of 44.44%–100% was found for both sensitivity and specificity in 1.5 T MRI studies. A study[50] compared all single sequences and found that T2w and TOF provided the most accurate information (both 100% accuracy). However, another study[45] investigated different types of T1w and found that 2D-CSE and 3D-FSE showed the best results (both sensitivity 95.7% and specificity 100%). Mean sensitivity (89%) and specificity (87%) values showed very good diagnostic accuracy of 1.5 T MRI for the detection of unstable plaque. Detailed information is listed in Table 10.

OTHER CHARACTERISTICS. The last category included only characteristics investigated by a single study (comparison) on

TABLE 7. Diagnostic Accuracy of MRI in Detection of Neovascularization

First Author	Specific Sequences	Number of Patients	Number in Analysis	Plaque Characteristic (MRI)	Plaque Characteristic (Histology)	Sensitivity (%)	Specificity (%)
Neovascularization—1.5 Tesla							
Kawahara 2007b[35]	T1w (CE-MRI)	9	10	Enhancement patterns	Microvessels	85.71	100
Yuan 2002[40]	TOF, T1w, CE-MRI	20	178	>80% signal intensity increase (enhancement)	Neovascularization	76.00	79.20
Neovascularization—3.0 Tesla							
Millon 2012d[30]	TOF, T1w, PDw, CE-MRI	59	59	Enhancement	Neovascularization	77.78	69.57

PD = proton dense; TOF = time of flight; CE-MRI = contrast enhanced magnetic resonance imaging.

15222586, 2025, 3, Downloaded from https://onlinelibrary.wiley.com/doi/10.1002/jmri.29522, Wiley Online Library on [04/09/2026]. See the Terms and Conditions (https://onlinelibrary.wiley.com/terms-and-conditions) on Wiley Online Library for rules of use; OA articles are governed by the applicable Creative Commons License

TABLE 8. Diagnostic Accuracy of MRI in Detection of Inflammation

First Author	Specific Sequences	Number of Patients	Number in Analysis	Plaque Characteristic (MRI)	Plaque Characteristic (Histology)	Sensitivity (%)	Specificity (%)
Inflammation—1.5 Tesla							
Kawahara 2008[27]	3D GRASS (CE-MRI)	10	10	SPIO uptake	Presence of macrophages	62.50	100
Papini 2011[37]	FLASH GRE (CE-MRI)	22	22	Enhancement	Inflammation	77.78	84.62
Inflammation—3.0 Tesla							
Millon 2012e[30]	TOF, T1w, PDw, CE-MRI	59	59	Enhancement	Inflammation (macrophages)	69.23	60.00

PD = proton dense; TOF = time of flight; CE-MRI = contrast enhanced magnetic resonance imaging; GRASS = gradient recalled acquisition in the steady state; FLASH = fast low angle shot; GRE = gradient echo; SPIO = superparamagnetic particles of iron oxide.

1.5 T MRI listed in Table 11—AHA plaque type I–II, AHA plaque type III, and hard plaque. The first two characteristics represent fatty streak and pre-atheromatous lesions with extracellular lipid pools and show near-normal wall thickness, challenging to detect by MRI. However, it was detected in one study with good sensitivity (66.67%–81.08%) and very high specificity (98.14%–100%).[51] Hard plaque was detected with high sensitivity (92.86%) and specificity (100%).[52]

Finally, an overview of proposed imaging criteria for MRI detection of specific characteristics according to the highest accuracy results in retrieved studies is provided in Table 12.

Discussion

The results of our diagnostic test accuracy systematic review showed that MRI detected carotid plaque composition with a high level of tissue discrimination allowing the differentiation between 13 specific plaque characteristics. MRI proved to have high diagnostic accuracy for detection of calcification (3 T MRI: mean sensitivity 92%/mean specificity 90%; 1.5 T MRI: mean sensitivity 81%/mean specificity 91%), fibrous cap (1.5 T: 89%/87%), unstable plaque (1.5 T: 89%/87%), IPH (1.5 T: 86%/88%), and LRNC (1.5 T: 89%/79%).

Regarding calcification, CT is considered the superior modality for its detection.[53,54] A direct comparison of MRI and CT showed that the calcification volume based on MRI is smaller than those obtained with CT.[55] However, in our systematic review we found that MRI had a high diagnostic accuracy for the calcification imaging in 1.5 T and 3 T MRI among all other characteristics recovered. Therefore, MRI could represent a reliable test to detect calcifications. To notice, calcification is considered a protective risk factor for stroke,[56] but its impact on plaque rupture has also been described.[57]

The fibrous cap, which typically covers a large LRNC and provides essential protection against clinical consequences of atherosclerosis,[58] was accurately detected by MRI with the capability of distinguishing intact/thick fibrous cap from intact thin and ruptured cap.[26] In particular, the ruptured cap is strongly related to a recent stroke,[8] 23 times more likely compared to thick fibrous caps.[59]

High-risk unstable plaque, common in asymptomatic patients and closely associated with stroke, typically consists of IPH, LRNC, ulceration or thin/ruptured fibrous cap,[9,45,60] was also detected by 1.5 T MRI with high diagnostic accuracy. In direct comparison to US and CT, MRI showed the highest diagnostic accuracy compared to US and CT.[6,61]

Regarding IPH detection, MPRAGE imaging remains the most reliable and accurate technique in 1.5 T based on extracted accuracies, where several sequences showed similar diagnostic accuracy in 3 T, proving not to be a superior

15222586, 2025, 3, Downloaded from https://onlinelibrary.wiley.com/doi/10.1002/jmri.29522, Wiley Online Library on [04/09/2026]. See the Terms and Conditions (https://onlinelibrary.wiley.com/terms-and-conditions) on Wiley Online Library for rules of use; OA articles are governed by the applicable Creative Commons License

TABLE 9. Diagnostic Accuracy of MRI in Detection of Loose Matrix

First Author	Specific Sequences	Number of Patients	Number in Analysis	Plaque Characteristic (MRI)	Plaque Characteristic (Histology)	Sensitivity (%)	Specificity (%)
Loose matrix—1.5 Tesla							
Saam 2005g[46]	T1w, T2w, PDw, TOF	31	214	Hyperintense: T2w/PDw, iso/hyperintense: T1w, isointense: TOF	Loose matrix (all areas)	64.42	71.82
Saam 2005h[46]	T1w, T2w, PDw, TOF	31	214	Hyperintense: T2w/PDw, iso/hyperintense: T1w, isointense: TOF	Loose matrix (areas >2 mm^2)	78.79	77.03
Loose matrix—3.0 Tesla							
Dai 2017g[23]	MATCH	46	298	T2w: hyperintense; hyper-T1w: isointense	Loose matrix	90.90	75.90
Dai 2017h[23]	T1w, T2w, PDw, TOF	46	298	T2w/PDw: hyperintense; TOF: isointense; T1w: hypo/isointense	Loose matrix	81.80	93.10
Millon 2012f[30]	TOF, T1w, PDw, CE-MRI	59	59	Enhancement	Loose matrix (loose fibrosis)	81.82	69.23
Qiao H 2020d[22]	3D T1w mapping GOAL-SNAP	19	52	Mean T1 value of loose matrix	Loose matrix	79.20	42.90

PD = proton dense; TOF = time of flight; CE-MRI = contrast enhanced magnetic resonance imaging; MATCH = multicontrast atherosclerosis characterization; GOAL-SNAP = simultaneous noncontrast angiography and intraplaque hemorrhage imaging with 3D golden angle radial k-space sampling.

15222586, 2025, 3, Downloaded from https://onlinelibrary.wiley.com/doi/10.1002/jmri.29522, Wiley Online Library on [04/09/2026]. See the Terms and Conditions (https://onlinelibrary.wiley.com/terms-and-conditions) on Wiley Online Library for rules of use; OA articles are governed by the applicable Creative Commons License

TABLE 10. Diagnostic Accuracy of MRI in Detection of Unstable Plaque

First Author	Specific Sequences	Number of Patients	Number in Analysis	Plaque Characteristic (MRI)	Plaque Characteristic (Histology)	Sensitivity (%)	Specificity (%)
Unstable plaque—1.5 Tesla							
Cappendijk 2005a[60]	T2w, T1w, interm.-w; part-T2w, 3D T1w	11	79	Vulnerable plaque (hemorrhage and/or lipid core)—qualitative	Hemorrhage and/or lipid core/ vulnerable plaque	93.10	96.00
Cappendijk 2005b[60]	T2w, T1w, interm.-w; part-T2w, 3D T1w	11	79	Vulnerable plaque (hemorrhage and/or lipid core)—semiquantitative	Hemorrhage and/or lipid core/ vulnerable plaque	75.86	100
Honda 2006c[50]	2D TOF	17	18	High signal intensity	Complicated plaque—Class >IV	100	100
Honda 2006d[50]	PDw	17	18	High signal intensity	Complicated plaque—Class >IV	44.44	55.56
Honda 2006e[50]	T1w	17	18	High signal intensity	Complicated plaque—Class >IV	100	44.44
Honda 2006f[50]	T2w	17	16	High signal intensity	Complicated plaque—Class >IV	100	100
Lukanova 2015d[6]	T1w, T2w/PDw, CE-MRI	25	30	Unstable plaque (AHA type IV-V and VI) for MRI	Soft unstable plaque (LRNC and/or IPH with <70% of fibrous tissue/ calcification)	100	88.89
Moody 2003[91]	MPRAGE	63	63	Hypersignal	Complicated plaque (AHA type VI)	84.09	84.21
Narumi 2017d[45]	T1w 2D-CSE	35	35	AHA type IV-V and VI for MRI	Vulnerable plaque (AHA type IV-V + VI)	95.70	100
Narumi 2017e[45]	T1w 2D-FSE	35	35	AHA type IV-V and VI for MRI	Vulnerable plaque (AHA type IV-V + VI)	82.60	100
Narumi 2017f[45]	T1w 3D-FSE	35	35	AHA type IV-V and VI for MRI	Vulnerable plaque (AHA type IV-V + VI)	95.70	100
Puppini 2006e[86]	TOF, T1w, T2w, PDw	15	56	Hyper-isointense (T1w/TOF), variable (T2w/PDw)	Lipid core and/or hemorrhage	93.75	100

15222586, 2025, 3, Downloaded from https://onlinelibrary.wiley.com/doi/10.1002/jmri.29522, Wiley Online Library on [04/09/2026]. See the Terms and Conditions (https://onlinelibrary.wiley.com/terms-and-conditions) on Wiley Online Library for rules of use; OA articles are governed by the applicable Creative Commons License

TABLE 10. Continued

First Author	Specific Sequences	Number of Patients	Number in Analysis	Plaque Characteristic (MRI)	Plaque Characteristic (Histology)	Sensitivity (%)	Specificity (%)
Takemoto 2013e[87]	T1w	69	71	Plaque/muscle ratio cut-off 1.18>	Complicated plaque (AHA type VI)	85.70	59.10
Watanabe 2008[61]	TOF, T1w, T2w	54	54	High signal intensity (T2w; cat. A); high signal intensity (T1w; cat. B)	At-risk soft plaque	95.83	93.33
Yoshida 2005a[52]	T1w, T2w	22	22	Markedly high signal (at least at one sequence)	Soft plaque	100	92.86
Yoshida 2008[92]	3D T1w, T1w, T2w	66	66	Mean relative overall signal intensity—cutoff 1.25 for soft plaque	Soft plaque	84.38	79.41
Yuan 2001b[49]	T1w, T2w, PDw, TOF	18	90	Hyper/isointense (T1w/ TOF), hypo/isointense (PDw/T2w)	Soft plaque (lipid core/acute hemorrhage)	84.85	91.67
Unstable plaque—3.0 Tesla							
Millon 2012g[30]	TOF, T1w, PDw, CE-MRI	59	59	Enhancement	Vulnerable plaque (Lovett grade 3–4)	79.49	80.00
Millon 2012h[30]	TOF, T1w, PDw, CE-MRI	59	59	Enhancement	Vulnerable plaque (AHA type VI)	80.00	55.88

PD = proton dense; AHA = American Heart Association; TOF = time of flight; CE-MRI = contrast enhanced magnetic resonance imaging.

15222586, 2025, 3, Downloaded from https://onlinelibrary.wiley.com/doi/10.1002/jmri.29522, Wiley Online Library on [04/09/2026]. See the Terms and Conditions (https://onlinelibrary.wiley.com/terms-and-conditions) on Wiley Online Library for rules of use; OA articles are governed by the applicable Creative Commons License

TABLE 11. Diagnostic Accuracy of MRI in Detection of Other Characteristics

First Author	Specific Sequences	Number of Patients	Number in Analysis	Plaque Characteristic (MRI)	Plaque Characteristic (Histology)	Sensitivity (%)	Specificity (%)
Other characteristics—1.5 Tesla							
Cai 2002e[51]	T1w; PDw; T2w; TOF	60	252	Indistinguishable from near-normal carotid wall	AHA plaque type I-II	66.67	100
Cai 2002f[51]	T1w; PDw	60	252	Focal, slightly high signals in some cases	AHA plaque type III	81.08	98.14
Yoshida 2005b[52]	T1w, T2w	22	22	Low to equal signal (both sequences)	Hard plaque	92.86	100

PD = proton dense; AHA = American Heart Association; TOF = time of flight.

technique based on accuracy. Furthermore, the MATCH sequence provided a significantly higher signal-contrast ratio for IPH compared to the conventional multi-contrast protocol.[23,62] IPH represents not only the characteristic most associated with stroke but also a factor accelerating plaque progression,[63] whose higher frequency is associated with use of antithrombotic treatment.[64] MRI is the imaging modality of choice for IPH detection based on the magnetic properties of hemoglobin and the ability to stage IPH as fresh, recent, and old.[43,44]

Regarding LRNC, which tends to be present in plaques associated with thrombotic complications[65] and a high risk of stroke recurrence (HR 2.73),[66] the same high sensitivity was found in 1.5 T MRI as for the detection of the fibrous cap, usually covering the LRNC. Whereas CT struggles in the differentiation of LRNC from IPH because both exhibit similar CT attenuation,[67] MRI proved to be the optimal imaging modality for the identification and quantification of LRNC. Importantly, LRNC represents together with IPH the best indicators of lesion severity currently visualized by carotid MRI.[68] Regarding IPH and LRNC detection, 3 T studies showed lower accuracy compared to 1.5 T machines. A previous study has shown a good agreement between the two field strengths for calcification and LRNC. However, the agreement for IPH was slightly different with better performance at 1.5 T than 3 T,[69] confirmed by another study.[70] At higher field strengths, the increased susceptibility of calcification and paramagnetic ferric iron in IPH may alter the quantification and detection of such characteristics. Moreover, motion, local fat-saturation failure, and flow artifacts had a higher impact on the degradation of 3 T image quality compared to 1.5 T.[69,70] Also, improved coils and new sequences at 3 T have been developed over the last few years to increase the detection of IPH and LRNC.[22,25,28,71,72] Thus, another explanation could be the heterogeneous use of advanced techniques and sequences (T2w and T1w mapping, CS-3D MERGE, SNAP, etc.) in the included studies despite their good accuracy. Further studies are needed to directly compare the diagnostic accuracy of 1.5 T to 3 T advanced sequences with histological evaluation as the reference standard.

Regarding other characteristics detected by MRI with good accuracy, fibrous plaque represents plaque stability with no thromboembolic protentional[73] and in particular T2w mapping more accurately detected fibrous plaque and quantified LRNC.[25] For detection of ulceration which represents an important risk factor of stroke,[74] CT is considered the first-line noninvasive modality with the highest accuracy confirmed in direct comparison with MRI and US.[6] However, CE-MRI has the advantage of ulceration detection also in calcified plaques, which remains one of the CT limitations.[75]

Intraplaque neovascularization is considered to be crucial in the genesis of IPH caused by ruptured neovessels.[76]

15222586, 2025, 3, Downloaded from https://onlinelibrary.wiley.com/doi/10.1002/jmri.29522, Wiley Online Library on [04/09/2026]. See the Terms and Conditions (https://onlinelibrary.wiley.com/terms-and-conditions) on Wiley Online Library for rules of use; OA articles are governed by the applicable Creative Commons License

TABLE 12. Evaluation of Carotid Plaque Characteristics by MRI (1.5–3 T) Based on the Highest-Accurate Results From Retrieved Studies in Our Systematic Review (NA for Fibrous Plaque Due to Ununited and Heterogenous Imaging Criteria in Published Studies)

	Preferred Sequence	T1w	T2w	PDw	TOF	CE-MRI	Importance of CE-MRI	Evidence
IPH	MPRAGE	Hyper					−	+++
Fresh IPH	Multisequence	Hyper	Iso/hypo	Iso/hypo	Hyper		−	+
Recent IPH	Multisequence	Hyper	Hyper	Hyper	Hyper		−	+
Old IPH	Multisequence	Hypo	Hypo	Hypo	Hypo		−	+
LRNC	Multisequence	Hyper/iso	Iso/hypo	Iso/hypo	Hyper/iso		−	+++
Calcification	Multisequence, MERGE	Marked hypo	Marked hypo	Marked hypo	Marked hypo		−	+++
Fibrous cap	TOF, CE-MRI				Hypo band	Hypo band	±	+++
Ulceration	TOF, CE-MRI				Surface disruption	Surface disruption	±	++
Neovascularization	CE-MRI					CE	+	+
Inflammation	CE-MRI					CE	+	+
Loose matrix	Multisequence, MATCH	Iso/hypo	Hyper	Hyper	Iso		−	+

Level of evidence: based on the number and homogeneity of retrieved studies as "+++" (very strong level of evidence), "++" (strong), "+" (moderate). Importance of CE-MRI: based on the evidence from retrieved studies as "+" (high benefit in increasing diagnostic accuracy compared to non-enhanced examination), "±" (no evidence of high benefit but can be useful), and "–" (no benefit). PD = proton dense; TOF = time of flight; CE-MRI = contrast enhanced magnetic resonance imaging; MATCH = multicontrast atherosclerosis characterization; MPRAGE = magnetization prepared rapid gradient echo; MERGE = motion-sensitized driven equilibrium prepared rapid gradient echo.

15222586, 2025, 3, Downloaded from https://onlinelibrary.wiley.com/doi/10.1002/jmri.29522, Wiley Online Library on [04/09/2026]. See the Terms and Conditions (https://onlinelibrary.wiley.com/terms-and-conditions) on Wiley Online Library for rules of use; OA articles are governed by the applicable Creative Commons License

Neovascularization and inflammation represent structural changes in intraplaque content that are not conclusively associated with stroke and CE-US remains the modality of choice for their detection followed by CE-MRI.[77] In contrast, loose matrix, considered as plaque healing or fibrosis loose revealing prone to rupture plaque, can only be detected by MRI.[30]

Finally, we found a mean sensitivity of 89% and specificity of 87% values showing very good diagnostic accuracy of 1.5 T MRI for the detection of unstable plaque (80% sensitivity for 3 T). Given that unstable plaques play a key role in the risk for major cardiovascular events,[9] the purpose of our study was to determine the diagnostic accuracy (sensitivity and specificity) of MRI for detection of such unstable carotid plaques compared to histology. Our results assessed the highest sensitivity and specificity of MRI for detection of unstable carotid plaques and their histological components providing shreds of evidence that consolidate its place in the patient's workup. The strength of our analysis is the large number of included studies and to the best of our knowledge, this is the first comprehensive study investigating the diagnostic accuracy of MRI in the detection of carotid plaques morphology. Calcification, LRNC, and IPH are the most prevalent plaque characteristics in a population >70 years[78] and current guidelines suggest that the composition of carotid plaque is crucial for future stroke risk and for determining possible surgical intervention benefits based on plaque instability.[79] MRI has been shown to be a cost-effective tool for identifying those patients,[80] which confirmed the need for accurate plaque imaging and the usefulness of systematic follow-up of patients at risk who can benefit from different therapeutic strategies or interventional treatments.

The limitations of our systematic review included: 1) The lack of standardization for MRI imaging of specific plaque characteristics that resulted in a large heterogeneity in the definitions of MRI characteristics in the retrieved studies. The heterogeneity of definitions (eg, fibrous plaque, loose matrix, or unstable plaque) implies that a subset of these studies would not be likely to provide valuable information and might have negatively affected the estimation of the diagnostic accuracy; 2) A long period of study publications, but no significant changes in sensitivity and specificity were found over time for both 1.5 T and 3 T studies (Figs. S1 and S2 in the Supplemental Material); 3) A small number of studies or a limited number of patients in included studies that investigated some characteristics by MRI should be taken into account.

In future directions, deep learning might play a key role in improving the diagnostic accuracy of MRI in the detection of plaque features and helping assess stroke risk.[81] An improvement of specific sequences by increasing resolution and decreasing time is needed using dedicated coils and novel sequences such as MATCH, MERGE, or DANTE, and techniques such as T1w and T2w mapping.

In conclusion, we showed a high diagnostic accuracy of MRI that was able to detect a high number of plaque characteristics regardless of the strength of the magnets (1.5 T or 3 T). These results emphasize the role of MRI as the first-line imaging modality for complex assessment of carotid plaque morphology, particularly regarding high-risk characteristics of instability. MRI of plaques is therefore likely to be useful for patient risk stratification to guide management and follow-up of the drugs' effect on carotid plaque composition, particularly in clinical trials and prospective longitudinal studies investigating plaque progression and regression.

Acknowledgments

We are very thankful to Aristeidis H. Katsanos for his valuable help with the study design; to Karen Von Deneen, Di Dong, and Yukari Yamada for translation of Chinese and Japanese articles; and to Šárka Kostecká and Cecile Jaques for searching the full-texts of articles. The authors received no financial support for the research, authorship, and/or publication of this article. David Pakizer was supported by the VIA PhD grant of the University of Ostrava for travel related to this analysis and by the Moravian-Silesian Region for his PhD study (scholarship grant no. 00736/2023/RRC).

Conflict of Interest

The authors declared no potential conflicts of interest.

References

1. Feeley TM, Leen EJ, Colgan MP, Moore DJ, Hourihane DO'B, Shanik GD. Histologic characteristics of carotid artery plaque. J Vasc Surg 1991;13(5):719-724.
2. Lusis AJ. Atherosclerosis. Nature 2000;407(6801):233-241.
3. Traub O, Berk BC. Laminar shear stress. Arterioscler Thromb Vasc Biol 1998;18(5):677-685.
4. Arroyo L. Mechanisms of plaque rupture mechanical and biologic interactions. Cardiovasc Res 1999;41(2):369-375.
5. Kerwin WS, Hatsukami T, Yuan C, Zhao XQ. MRI of carotid atherosclerosis. Am J Roentgenol 2013;200(3):W304-W313.
6. Lukanova DV, Nikolov NK, Genova KZ, Stankev MD, Georgieva EV. The accuracy of noninvasive imaging techniques in diagnosis of carotid plaque morphology. Open Access Maced J Med Sci 2015;3(2):224-230.
7. Toussaint JF, LaMuraglia GM, Southern JF, Fuster V, Kantor HL. Magnetic resonance images lipid, fibrous, calcified, hemorrhagic, and thrombotic components of human atherosclerosis in vivo. Circulation 1996;94(5):932-938.
8. Gupta A, Baradaran H, Schweitzer AD, et al. Carotid plaque MRI and stroke risk. Stroke 2013;44(11):3071-3077.
9. Kamtchum-Tatuene J, Noubiap JJ, Wilman AH, Saqqur M, Shuaib A, Jickling GC. Prevalence of high-risk plaques and risk of stroke in patients with asymptomatic carotid stenosis. JAMA Neurol 2020;77(12):1524-1535.
10. Schindler A, Schinner R, Altaf N, et al. Prediction of stroke risk by detection of hemorrhage in carotid plaques. JACC Cardiovasc Imaging 2020;13(2):395-406.

15222586, 2025, 3, Downloaded from https://onlinelibrary.wiley.com/doi/10.1002/jmri.29522, Wiley Online Library on [04/09/2026]. See the Terms and Conditions (https://onlinelibrary.wiley.com/terms-and-conditions) on Wiley Online Library for rules of use; OA articles are governed by the applicable Creative Commons License

11. Page MJ, McKenzie JE, Bossuyt PM, et al. The PRISMA 2020 statement: An updated guideline for reporting systematic reviews. BMJ 2021;372:n71.
12. Cohen JF, Korevaar DA, Altman DG, et al. STARD 2015 guidelines for reporting diagnostic accuracy studies: Explanation and elaboration. BMJ Open 2016;6(11):e012799.
13. Pakizer D, Sirimarco G, Elmers J, et al. Search strategies related to: Sensitivity and specificity of atherosclerotic plaque components in carotid arteries detectable by CT, MRI, PET, and sonography – Comparison with histology: A systematic review and meta-analysis (version 1). Zenodo 2022. https://doi.org/10.5281/zenodo.7229512.
14. Liberopoulos K, Kaponis A, Kokkinis K, et al. Comparative study of magnetic resonance angiography, digital subtraction angiography, duplex ultrasound examination with surgical and histological findings of atherosclerotic carotid bifurcation disease. Int Angiol 1996;15(2):131-137.
15. Albuquerque LC, Narvaes LB, Maciel AA, et al. Intraplaque hemorrhage assessed by high-resolution magnetic resonance imaging and C-reactive protein in carotid atherosclerosis. J Vasc Surg 2007;46(6):1130-1137.
16. Altaf N, Akwei S, Auer DP, MacSweeney ST, Lowe J. Magnetic resonance detected carotid plaque hemorrhage is associated with inflammatory features in symptomatic carotid plaques. Ann Vasc Surg 2013;27(5):655-661.
17. Du Y, Yang L, Wang Y, Zhao Y, Li D, Yu W. Carotid intraplaque hemorrhage imaging using MRI: Comparison of the diagnostic performance between multi-contrast atherosclerosis characterization and magnetization-prepared rapid acquisition gradient-echo with histology. Chin J Radiol 2017;51(6):412-416.
18. Li D, Qiao H, Han Y, et al. Histological validation of simultaneous non-contrast angiography and intraplaque hemorrhage imaging (SNAP) for characterizing carotid intraplaque hemorrhage. Eur Radiol 2021;31(5):3106-3115.
19. Ota H, Tamura H, Itabashi R, et al. Quantitative characterization of carotid plaque components using MR apparent diffusion coefficients and longitudinal relaxation rates at 3T: A comparison with histology. J Magn Reson Imaging 2018;48(6):1657-1667.
20. Ota H, Yarnykh VL, Ferguson MS, et al. Carotid intraplaque hemorrhage imaging at 3.0-T MR imaging: Comparison of the diagnostic performance of three T1-weighted sequences. Radiology 2010;254(2):551-563.
21. Liu J, Sun J, Balu N, et al. Semiautomatic carotid intraplaque hemorrhage volume measurement using 3D carotid MRI. J Magn Reson Imaging 2019;50(4):1055-1062.
22. Qiao H, Li D, Cao J, et al. Quantitative evaluation of carotid atherosclerotic vulnerable plaques using in vivo T1 mapping cardiovascular magnetic resonaonce: Validation by histology. J Cardiovasc Magn Reson 2020;22(1):1-11.
23. Dai Y, Lv P, Lin J, et al. Comparison study between multicontrast atherosclerosis characterization (MATCH) and conventional multicontrast MRI of carotid plaque with histology validation. J Magn Reson Imaging 2017;45(3):764-770.
24. Young VE, Patterson AJ, Sadat U, et al. Diffusion-weighted magnetic resonance imaging for the detection of lipid-rich necrotic core in carotid atheroma in vivo. Neuroradiology 2010;52(10):929-936.
25. Chai JT, Biasiolli L, Li L, et al. Quantification of lipid-rich core in carotid atherosclerosis using magnetic resonance T2 mapping. JACC Cardiovasc Imaging 2017;10(7):747-756.
26. Hatsukami TS, Ross R, Polissar NL, Yuan C. Visualization of fibrous cap thickness and rupture in human atherosclerotic carotid plaque in vivo with high-resolution magnetic resonance imaging. Circulation 2000;102(9):959-964.
27. Kawahara I, Nakamoto M, Kitigawa N, et al. Potential of magnetic resonance plaque imaging using superparamagnetic particles of iron oxide for the detection of carotid plaque. Neurol Med Chir 2008;48(4):157-162.
28. Dong L, Li B, Wang Z, Lu D, Wang Y, Zhang Z. Feasibility study of rapid three dimensional MR angiography in visualization of carotid atherosclerotic plaque. Chin J Radiol 2017;51(4):299-303.
29. D'Onofrio M, Mansueto G, Faccioli N, et al. Doppler ultrasound and contrast-enhanced magnetic resonance angiography in assessing carotid artery stenosis. Radiol Med 2006;111(1):93-103.
30. Millon A, Boussel L, Brevet M, et al. Clinical and histological significance of gadolinium enhancement in carotid atherosclerotic plaque. Stroke 2012;43(11):3023-3028.
31. Millon A, Mathevet JL, Boussel L, et al. High-resolution magnetic resonance imaging of carotid atherosclerosis identifies vulnerable carotid plaques. J Vasc Surg 2013;57(4):1046-1051.
32. Sigovan M, Bidet C, Bros S, et al. 3D black blood MR angiography of the carotid arteries. A simple sequence for plaque hemorrhage and stenosis evaluation. Magn Reson Imaging 2017;42:95-100.
33. Wang Z, Fan Z, Liu W, et al. Incremental diagnostic value of neck vessel wall imaging technique with T1-weighted three-dimensional variable-flip-angle turbo spin-echo before revascularization in patients with carotid atherosclerotic disease. Chin J Radiol 2019;53(8):661-667.
34. Yim YJ, Choe YH, Ko Y, et al. High signal intensity halo around the carotid artery on maximum intensity projection images of time-of-flight MR angiography: A new sign for intraplaque hemorrhage. J Magn Reson Imaging 2008;27(6):1341-1346.
35. Kawahara I, Morikawa M, Honda M, et al. High-resolution magnetic resonance imaging using gadolinium-based contrast agent for atherosclerotic carotid plaque. Surg Neurol 2007;68(1):60-65.
36. Qiao Y, Etesami M, Malhotra S, et al. Identification of intraplaque hemorrhage on MR angiography images: A comparison of contrast-enhanced mask and time-of-flight techniques. Am J Neuroradiol 2011;32(3):454-459.
37. Papini GDE, Di Leo G, Tritella S, et al. Evaluation of inflammatory status of atherosclerotic carotid plaque before thromboendarterectomy using delayed contrast-enhanced subtracted images after magnetic resonance angiography. Eur J Radiol 2011;80(3):e373-e380.
38. Wang Q, Wang Y, Cai J, et al. Oblique-sagittal black-blood contrast-enhanced magnetic resonance imaging in preoperative evaluation for carotid endarterectomy. Nan Fang Yi Ke Da Xue Xue Bao 2011;31(3):385-391.
39. Yu W, Underhill HR, Ferguson MS, et al. The added value of longitudinal black-blood cardiovascular magnetic resonance angiography in the cross sectional identification of carotid atherosclerotic ulceration. J Cardiovasc Magn Reson 2009;11(1):1-10.
40. Yuan C, Kerwin WS, Ferguson MS, et al. Contrast-enhanced high resolution MRI for atherosclerotic carotid artery tissue characterization. J Magn Reson Imaging 2002;15(1):62-67.
41. Ideguchi R, Uetani M, Morikawa M, et al. Usefulness of dynamic contrast-enhanced MR imaging study for carotid atherosclerotic plaque. Jpn J Clin Radiol 2009;54(9):1119-1124.
42. Tapis P, El-Koussy M, Hewer E, Mono ML, Reinert M. Plaque vulnerability in patients with high- and moderate-grade carotid stenosis – Comparison of plaque features on MRI with histopathological findings. Swiss Med Wkly 2020;150:w20174.
43. Chu B, Kampschulte A, Ferguson MS, et al. Hemorrhage in the atherosclerotic carotid plaque: A high-resolution MRI study. Stroke 2004;35(5):1079-1084.
44. Cappendijk VC, Cleutjens KBJM, Heeneman S, et al. In vivo detection of hemorrhage in human atherosclerotic plaques with magnetic resonance imaging. J Magn Reson Imaging 2004;20(1):105-110.
45. Narumi S, Sasaki M, Miyazawa H, et al. T1-weighted magnetic resonance carotid plaque imaging: A comparison between conventional and fast spin-Echo techniques. J Stroke Cerebrovasc Dis 2017;26(2):273-279.
46. Saam T, Ferguson MS, Yarnykh VL, et al. Quantitative evaluation of carotid plaque composition by in vivo MRI. Arterioscler Thromb Vasc Biol 2005;25(1):234-239.

15222586, 2025, 3, Downloaded from https://onlinelibrary.wiley.com/doi/10.1002/jmri.29522, Wiley Online Library on [04/09/2026]. See the Terms and Conditions (https://onlinelibrary.wiley.com/terms-and-conditions) on Wiley Online Library for rules of use; OA articles are governed by the applicable Creative Commons License

47. Cappendijk VC, Heeneman S, Kessels AGH, et al. Comparison of single-sequence T1w TFE MRI with multisequence MRI for the quantification of lipid-rich necrotic core in atherosclerotic plaque. J Magn Reson Imaging 2008;27(6):1347-1355.

48. Esposito L, Sievers M, Sander D, et al. Detection of unstable carotid artery stenosis using MRI. J Neurol 2007;254(12):1714-1722.

49. Yuan C, Mitsumori LM, Beach KW, Maravilla KR. Carotid atherosclerotic plaque: Noninvasive MR characterization and identification of vulnerable lesions. Radiology 2001;221(2):285-299.

50. Honda M, Kitagawa N, Tsutsumi K, Nagata I, Morikawa M, Hayashi T. High-resolution magnetic resonance imaging for detection of carotid plaques. Neurosurgery 2006;58(2):338-346.

51. Cai JM, Hatsukami TS, Ferguson MS, Small R, Polissar NL, Yuan C. Classification of human carotid atherosclerotic lesions with in vivo multicontrast magnetic resonance imaging. Circulation 2002;106(11):1368-1373.

52. Yoshida K, Goto M, Funaki T, et al. Noninvasive carotid plaque characterization by black blood MRI. No Shinkei Geka 2005;33(3):235-241.

53. Wintermark M, Jawadi SS, Rapp JH, et al. High-resolution CT imaging of carotid artery atherosclerotic plaques. Am J Neuroradiol 2008;29(5):875-882.

54. Schroeder S, Kuettner A, Leitritz M, et al. Reliability of differentiating human coronary plaque morphology using contrast-enhanced multislice spiral computed tomography. J Comput Assist Tomogr 2004;28(4):449-454.

55. Mujaj B, Lorza AMA, van Engelen A, et al. Comparison of CT and CMR for detection and quantification of carotid artery calcification: The Rotterdam study. J Cardiovasc Magn Reson 2017;19(1):28.

56. Homssi M, Saha A, Delgado D, et al. Extracranial carotid plaque calcification and cerebrovascular ischemia: A systematic review and meta-analysis. Stroke 2023;54(10):2621-2628.

57. Kan Y, He W, Ning B, Li H, Wei S, Yu T. The correlation between calcification in carotid plaque and stroke: Calcification may be a risk factor for stroke. Int J Clin Exp Pathol 2019;12(3):750-758.

58. Watson MG, Byrne HM, Macaskill C, Myerscough MR. A two-phase model of early fibrous cap formation in atherosclerosis. J Theor Biol 2018;456:123-136.

59. Yuan C, Zhang S, Polissar NL, et al. Identification of fibrous cap rupture with magnetic resonance imaging is highly associated with recent transient ischemic attack or stroke. Circulation 2002;105(2):181-185.

60. Cappendijk VC, Cleutjens KBJM, Kessels AGH, et al. Assessment of human atherosclerotic carotid plaque components with multisequence MR imaging: Initial experience. Radiology 2005;234(2):487-492.

61. Watanabe Y, Nagayama M, Suga T, et al. Characterization of atherosclerotic plaque of carotid arteries with histopathological correlation: Vascular wall MR imaging vs. color Doppler ultrasonography (US). J Magn Reson Imaging 2008;28(2):478-485.

62. Fan Z, Yu W, Xie Y, et al. Multi-contrast atherosclerosis characterization (MATCH) of carotid plaque with a single 5-min scan: Technical development and clinical feasibility. J Cardiovasc Magn Reson 2014;16(1):53.

63. Takaya N, Yuan C, Chu B, et al. Presence of intraplaque hemorrhage stimulates progression of carotid atherosclerotic plaques. Circulation 2005;111(21):2768-2775.

64. Mujaj B, Bos D, Muka T, et al. Antithrombotic treatment is associated with intraplaque haemorrhage in the atherosclerotic carotid artery: A cross-sectional analysis of the Rotterdam study. Eur Heart J 2018;39(36):3369-3376.

65. Redgrave JNE, Lovett JK, Gallagher PJ, Rothwell PM. Histological assessment of 526 symptomatic carotid plaques in relation to the nature and timing of ischemic symptoms. Circulation 2006;113(19):2320-2328.

66. Deng F, Mu C, Yang L, et al. Carotid plaque magnetic resonance imaging and recurrent stroke risk. Medicine 2020;99(13):e19377.

67. de Weert TT, Ouhlous M, Zondervan PE, et al. In vitro characterization of atherosclerotic carotid plaque with multidetector computed tomography and histopathological correlation. Eur Radiol 2005;15(9):1906-1914.

68. Underhill HR, Hatsukami TS, Fayad ZA, Fuster V, Yuan C. MRI of carotid atherosclerosis: Clinical implications and future directions. Nat Rev Cardiol 2010;7(3):165-173.

69. Underhill HR, Yarnykh VL, Hatsukami TS, et al. Carotid plaque morphology and composition: Initial comparison between 1.5- and 3.0-T magnetic field strengths. Radiology 2008;248(2):550-560.

70. McNally JS, Yoon HC, Kim SE, et al. Carotid MRI detection of intraplaque hemorrhage at 3T and 1.5T. J Neuroimaging 2015;25(3):390-396.

71. de Buck MHS, Jezzard P, Frost R, et al. 10-channel phased-array coil for carotid wall MRI at 3T. PLoS One 2023;18(8):e0288529.

72. Wang Y, Liu X, Wang J, et al. Simultaneous T1, T2, and T2* mapping of carotid plaque: The SIMPLE* technique. Radiology 2023;307(3):e222061.

73. Geroulakos G, Ramaswami G, Nicolaides A, et al. Characterization of symptomatic and asymptomatic carotid plaques using high-resolution real-time ultrasonography. Br J Surg 1993;80(10):1274-1277.

74. Smith LC, Funnell JP, Richards T, Best LMJ. Carotid plaque ulceration: Unquantified predictor of stroke. BJS Open 2023;7(3):zrad058.

75. Yuan J, Usman A, Das T, Patterson AJ, Gillard JH, Graves MJ. Imaging carotid atherosclerosis plaque ulceration: Comparison of advanced imaging modalities and recent developments. Am J Neuroradiol 2017;38(4):664-671.

76. Milei J, Parodi JC, Alonso GF, Barone A, Grana D, Matturri L. Carotid rupture and intraplaque hemorrhage: Immunophenotype and role of cells involved. Am Heart J 1998;136(6):1096-1105.

77. Saba L, Saam T, Jäger HR, et al. Imaging biomarkers of vulnerable carotid plaques for stroke risk prediction and their potential clinical implications. Lancet Neurol 2019;18(6):559-572.

78. Bos D, Arshi B, van den Bouwhuijsen QJA, et al. Atherosclerotic carotid plaque composition and incident stroke and coronary events. J Am Coll Cardiol 2021;77(11):1426-1435.

79. Naylor R, Rantner B, Ancetti S, et al. Editor's choice – European Society for Vascular Surgery (ESVS) 2023 Clinical Practice Guidelines on the Management of Atherosclerotic Carotid and Vertebral Artery Disease. Eur J Vasc Endovasc Surg 2023;65(1):7-111.

80. Gupta A, Mushlin AI, Kamel H, Navi BB, Pandya A. Cost-effectiveness of carotid plaque MR imaging as a stroke risk stratification tool in asymptomatic carotid artery stenosis. Radiology 2015;277(3):763-772.

81. Wang Y, Cai C, Du YM, et al. Assessment of stroke risk using MRI-VPD with automatic segmentation of carotid plaques and classification of plaque properties based on deep learning. J Radiat Res Appl Sci 2023;16(3):100630.

82. Bitar R, Moody AR, Leung G, et al. In vivo 3D high-spatial-resolution MR imaging of intraplaque hemorrhage. Radiology 2008;249(1):259-267.

83. Kampschulte A, Ferguson MS, Kerwin WS, et al. Differentiation of intraplaque versus juxtaluminal hemorrhage/thrombus in advanced human carotid atherosclerotic lesions by in vivo magnetic resonance imaging. Circulation 2004;110(20):3239-3244.

84. Saito H, Kuroda S, Hirata K, et al. Validity of dual MRI and ^{18}F-FDG PET imaging in predicting vulnerable and inflamed carotid plaque. Cerebrovasc Dis 2013;35(4):370-377.

85. Liu W, Xie Y, Wang C, et al. Atherosclerosis T1-weighted characterization (CATCH): Evaluation of the accuracy for identifying intraplaque hemorrhage with histological validation in carotid and coronary artery specimens. J Cardiovasc Magn Reson 2018;20(1):1-9.

86. Puppini G, Furlan F, Cirota N, et al. Characterisation of carotid atherosclerotic plaque: Comparison between magnetic resonance imaging and histology. Radiol Med 2006;111(7):921-930.

15222586, 2025, 3, Downloaded from https://onlinelibrary.wiley.com/doi/10.1002/jmri.29522, Wiley Online Library on [04/09/2026]. See the Terms and Conditions (https://onlinelibrary.wiley.com/terms-and-conditions) on Wiley Online Library for rules of use; OA articles are governed by the applicable Creative Commons License

87. Takemoto K, Ueba T, Takano K, et al. Quantitative evaluation using the plaque/muscle ratio index panels predicts plaque type and risk of embolism in patients undergoing carotid artery stenting. Clin Neurol Neurosurg 2013;115(8):1298-1303.

88. Honda M, Kawahara I, Kitagawa N, et al. Asymptomatic carotid artery plaques: Use of magnetic resonance imaging to characterize vulnerable plaques in 6 cases. Surg Neurol 2007;67(1):35-39.

89. Mitsumori LM, Hatsukami TS, Ferguson MS, Kerwin WS, Cai J, Yuan C. In vivo accuracy of multisequence MR imaging for identifying unstable fibrous caps in advanced human carotid plaques. J Magn Reson Imaging 2003;17(4):410-420.

90. Watanabe Y, Nagayama M, Sakata A, et al. Evaluation of fibrous cap rupture of atherosclerotic carotid plaque with thin-slice source images of time-of-flight MR angiography. Ann Vasc Dis 2014;7(2):127-133.

91. Moody AR, Murphy RE, Morgan PS, et al. Characterization of complicated carotid plaque with magnetic resonance direct thrombus imaging in patients with cerebral ischemia. Circulation 2003;107(24): 3047-3052.

92. Yoshida K, Narumi O, Chin M, et al. Characterization of carotid atherosclerosis and detection of soft plaque with use of black-blood MR imaging. Am J Neuroradiol 2008;29(5):868-874.

15222586, 2025, 3, Downloaded from https://onlinelibrary.wiley.com/doi/10.1002/jmri.29522, Wiley Online Library on [04/09/2026]. See the Terms and Conditions (https://onlinelibrary.wiley.com/terms-and-conditions) on Wiley Online Library for rules of use; OA articles are governed by the applicable Creative Commons License